Absolute Ionization Rates of Multielectron Transition Metal Atoms in Strong Infrared Laser Fields

Marc Smits,[1] C. A. de Lange,[1] Albert Stolow,[2,*] and D. M. Rayner[2,†]

[1]*Department of Physics and Astronomy, Vrije Universiteit Amsterdam, Netherlands*

[2]*Steacie Institute for Molecular Sciences, National Research Council Canada, 100 Sussex Drive, Ottawa, Ontario K1A 0R6 Canada*

(Received 31 May 2004; published 15 November 2004)

We report on nonresonant strong field ionization of the multielectron transition metal atoms V, Nb, Ta, Ni, and Pd. Operating in the adiabatic regime ($\lambda = 1.5$ μm), we quantitatively determined both (i) the first charge state saturation intensities and (ii) the absolute ionization rates for intensities ranging from threshold up to 3×10^{14} W/cm^2. We observed a dramatic suppression of ionization relative to single active electron approximation expectations. We suggest that this derives from dynamic polarization or screening effects within the multielectron atom, stressing a need for many-body theories of strong field ionization.

DOI: 10.1103/PhysRevLett.93.213003 PACS numbers: 32.80.Rm, 42.50.Hz

Strong field ionization dynamics is central to many extreme nonlinear optical processes such as high harmonic, x-ray, and attosecond pulse generation. Much of our understanding of these dynamics derives from adiabatic theories based upon strong field (SF) tunnel ionization and single active electron (SAE) approximations. These theories, of which Ammosov-Delone-Krainov (ADK) theory is a well known example [1], successfully describe the strong field ionization dynamics of the effectively SAE rare gas atoms [2]. To understand the strong field physics of matter more generally, true multielectron systems and their many-body dynamics must be considered. The first correlated two-electron phenomenon, nonsequential double ionization in rare gases, can be treated within the SF-SAE picture by considering the recollision of the continuum SAE with the core [2,3]. The strong field ionization of two-electron atoms (Mg and Ca) show perhaps the first hints of deviation from the SF-SAE picture [4,5]. More complex multielectron correlation phenomena, showing a complete failure of the SF-SAE picture, were observed in the strong field ionization of polyatomic molecules in both the adiabatic [6,7] and nonadiabatic [8,9] regimes. Diatomic molecules also show differences from SAE atoms that relate to the molecular nature of the physics [10–12]. A complete many-body theory treatment of multielectron dynamics in a strong laser field, however, is in the very early stages of development [13,14]. There is a great need for detailed, direct comparison of theory with simpler systems: multielectron atoms. We present a quantitative determination of absolute ionization rates as a function of intensity and saturation intensities for a series of such atoms.

In the adiabatic SF regime all electrons, not just the most weakly bound "active" one, must respond to the applied field. If there are many polarizable electrons, we expect that these will all be pushed by the field up against the partially suppressed barrier and lead to enhanced repulsion for the active electron, as was discussed for the case of molecules [8]. This type of dynamic polarization yields an effectively higher tunneling barrier and therefore a suppression of ionization. SAE models such as ADK appear to provide a good description of the ionization dynamics of the rare gases and, in this context, these show no suppression of ionization. To provide quantitative data on the adiabatic SF ionization dynamics of multielectron atoms, we have made a systematic study of two series of transition metal atoms: V, Nb, and Ta (five outer valence electrons), and Ni and Pd (ten outer valence electrons). We compare our results with both ADK theory and a simple model that we argue mimics the limiting behavior of infinitely polarizable systems: the delta or zero-range potential (ZRP).

A stable kHz-rate laser ablation source was used to produce the transition metal atomic beam, using helium as the carrier gas [15]. A rotating, translating rod of pure metal (V, Nb, Ta, Ni, Pd) was used as the target. An amplified fs Ti:Sa laser system pumped an optical parametric amplifier to produce <90 fs pulses at 1.5 μm with >150 μJ of energy [16]. The focused ($f/15$) infrared laser pulses intersected the atomic beam in the extraction region of a linear time-of-flight mass spectrometer. The mass spectrum and laser intensity were recorded for each laser shot. We measured the intensity dependence of the atomic mass peak up to a maximum of 3×10^{14} W/cm^2.

We implemented the saturation intensity method that employs a constant axial intensity ion collection geometry, as discussed in detail elsewhere [6,7]. Briefly, a 500 μmn slit perpendicular to the laser propagation direction permitted collection only of ions formed in a region of constant axial intensity. With this geometry, a linear dependence of the ionization yield on the logarithm of the intensity holds at high intensity. The saturation intensity, I_{sat}, is defined as the threshold intensity for this (extrapolated) linear behavior and is a general measure of

the "ease" of ionization. As I_{sat} is an atomic property which does not depend on experimental factors such as detection efficiency or focusing geometry, comparison with theory is unambiguous. Absolute laser intensities were determined by *in situ* calibration against the known saturation intensity of xenon, as described in detail elsewhere [7].

In Fig. 1 we show an example of a typical intensity scan, here for the Nb atom. Similar data were recorded for V, Ta, Ni, and Pd atoms. Saturation intensities are obtained by extrapolation of the high intensity linear behavior, as shown in the figure. The I_{sat} determined from each fit is given in Table I, along with the previously reported ionization potential [17] and static polarizability [18] of each atom.

The absolute ionization rates as a function of intensity were determined by transformation of the ion yield data as detailed elsewhere [7]. Briefly, the method depends on measuring the slope of the ion yield curve β. The cycle-averaged intensity dependent ionization rate is $W(I_0, f(t))$ where I_0 is the Gaussian peak intensity and $f(t)$ is the pulse envelope function. The time integral of this rate over the pulse envelope is given by

$$\int_{-\infty}^{\infty} W(I_0, f(t))dt = \ln\frac{\beta_\infty}{\beta_\infty - \beta}, \qquad (1)$$

where β_∞ is the slope associated with the limiting linear behavior at high intensity. The measurement of β_∞ provides an internal calibration of all unvaried experimental parameters [7]. For the case of a square-top pulse of duration τ, the integral $\int_{-\infty}^{\infty} W(I_0, f(t))dt$ reduces to $W(I_0)\tau$ where $W(I_0)$ is the absolute ionization rate. The slope β was obtained from the rise and run over its two neighboring points. To reduce differentiation noise, the raw ion yield data (as in Fig. 1) were first smoothed with a ten point binning method.

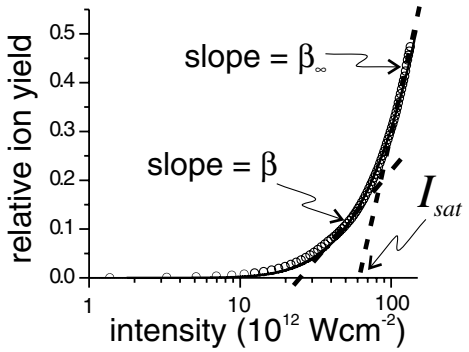

FIG. 1. A typical intensity scan, shown here for the Nb atom. The ion yield is plotted vs the logarithm of the peak intensity. A multiexponential fit to the data is shown as a solid line. The limiting slope β_∞, its intercept I_{sat}, and the slope β at a lower intensity are shown. As discussed in the text, β was used to extract the absolute ionization rates. All other atoms (not shown) were treated in a similar manner.

For the case of a square-top pulse of duration τ, the integral in Eq. (1) reduces to $W(I_0)\tau$ where $W(I_0)$ is the absolute ionization rate. In Fig. 2, both the square-top absolute ionization rate and the integrals $\int_{-\infty}^{\infty} W(I_0, f(t))dt$, are plotted as a function of absolute intensity for the atoms V, Nb, Ta, Ni, and Pd. The solid lines represent ionization rates derived from the gradients of the functional fits to the experimental data, demonstrated for Nb in Fig. 1. The effective pulse duration τ for the square-top pulse was obtained by fitting xenon intensity scan data to ADK theory.

We compare the observed ionization rates of the multielectron atoms with two limiting case models. The first model is ADK, a benchmark for SAE atoms. Our measurements are carried out at intensities where the Keldysh parameter, γ, ≈ 0.5 or less, conditions under which ADK is still expected to maintain good accuracy for cycle-averaged rates [19]. It can be seen from Table I that, in all cases, the experimental I_{sat} significantly exceeds the ADK value and from Fig. 2 that ADK drastically overestimates ionization rates: around the ADK I_{sat}, the ADK ionization rate is off by a factor of 10^4–10^6 (note that I_{sat} is a logarithmic measure). This demonstrates the dramatic nature of the suppression of ionization in these multielectron atoms relative to SAE expectations. More general, but more difficult to apply and therefore less widely used, treatments such as exact numerical SAE calculations [2] and the analytical SAE derivation of Perelomov-Popov-Terentev [20] show that ADK progressively underestimates ionization rates as γ increases above 0.5. This implies even greater disparity between our experimental results and the predictions of more sophisticated SAE approaches. We suggest that the suppression is due to the dynamic (but adiabatic) polarization of all electrons in the strong field, leading to displacement of electron density towards the barrier and, hence, increased repulsion for the active electron which must pass through this region in order to escape.

TABLE I. Experimental, ADK, and ZRP saturation intensities for V, Nb, Ta, Ni, and Pd. η, the relative measure of ZRP behavior, ranges from zero for ideal ADK behavior to one for ideal ZRP behavior. For reference, the electronic configurations, ionization potentials [17], and static polarizabilities [18] are given.

Atom	Configuration	IP (eV)	α Å^3	I_{sat} (10^{13}W/cm^2) Exp	ADK	ZRP	η
V	$[Ar]3d^3 4s^2$	6.75	12.4	3.2	1.2	12.2	0.18
Nb	$[Kr]4d^4 5s^1$	6.76	15.7	6.7	1.2	12.2	0.50
Ta	$[Xe]4f^{14} 5d^3 6s^2$	7.89	13.1	5.4	2.1	18.4	0.20
Ni	$[Ar]3d^8 4s^2$	7.6	6.8	4.7	1.8	16.7	0.19
Pd	$[Kr]4d^{10}$	8.34	4.8	6.2	2.6	21.3	0.19
Xe	$[Kr]4d^{10} 5s^2 5p^6$	12.13	4	9.5	9.5	57.6	0

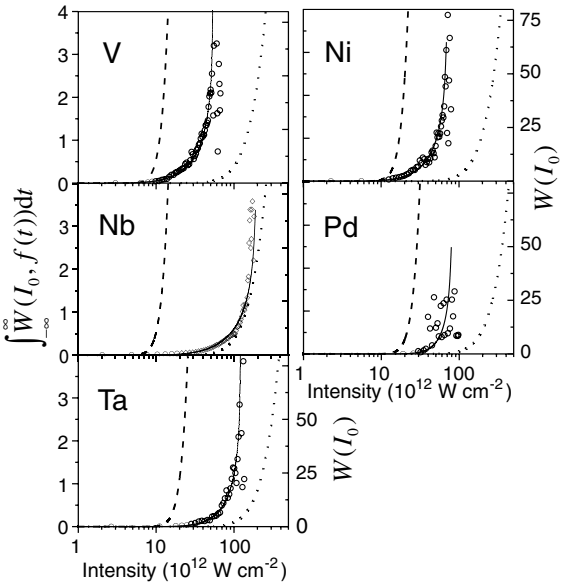

FIG. 2. Absolute ionization rates (open circles), determined from direct transformation [Eq. (1)] of ion yield data for V, Nb, Ta, Ni, and Pd. The envelope-integrated ionization rates, left ordinate, are plotted as a function of peak intensity. Assuming a square-top pulse, the resultant absolute ionization rates in ps^{-1} are given by the right ordinate. The solid lines are the same transformation applied to the numerical fits to the ion yield data. The dashed lines are the ionization rates obtained via ADK theory and show a dramatic overestimation of the rates. The dotted lines show the limiting behavior expected from a ZRP model.

Equivalently, a test charge approaching the barrier from afar climbs the potential due to the laser field and feels, at close range, enhanced repulsion due to the polarization of electrons towards the barrier and, therefore, an increase of the barrier height at short range (thus leading to dramatically reduced tunneling rates).

We now consider the other limiting case—that of very high multielectron contribution to the polarizability. None of the SAE models, including ADK, consider any dynamics internal to the potential and therefore cannot include dynamic screening effects. As full many-body theories of strong field ionization dynamics are still under development [13,14], it is useful to consider simplified models. Qualitatively, we expect an adiabatic multielectron polarization to lead to field-induced enhancement of the tunneling barrier for the active electron. As a model of the high polarizability limit, we used a simple function—the delta function or ZRP—which we argue represents the limiting case for high multielectron polarizability systems.

We expect that multielectron polarization leads to displacement of electron density away from the core in the direction of the laser electric field—i.e., downfield towards the tunneling barrier. This enhancement of electron density between the core and the exterior region should lead to enhanced screening of the core as viewed from the downfield exterior region. In the upfield region opposite the barrier, we expect, if anything, the core to be more exposed due to this displacement of electron density. As we are concerned with tunneling rates through the field-modified barrier, we focus only on the downfield side. A simple way to mimic multielectron screening is through the use of an effective Coulomb charge z. A reduced z implies core screening and leads to a change in the shape of the downfield potential relative to the $z = 1$ Coulomb potential, as illustrated in Fig. 3. The tunneling barrier increases as z decreases. In the limit $z \to 0$ (i.e.,"perfect" downfield screening), the potential tends to the triangular barrier associated with a delta, or zero-range, potential function in the field. If we neglect changes in the preexponential factor, we can estimate the tunneling rate through this limiting triangular barrier as that from a ZRP. We propose that the ZRP behaves as the high multielectron polarizability limit of dynamic screening of atoms in a strong laser field. Therefore, we used the cycle-averaged Wentzel-Kramers-Brillouin tunneling rates out of ZRPs as the second limiting case—that of high multielectron polarizability—for calculating ionization rates.

In Table I we present our experimental saturation intensities as well as the ADK and ZRP expectations. In Fig. 2, we show the absolute ionization rates calculated for each atom from both the ADK (dashed line) and ZRP (dotted line) models. In all cases, the experimental rates are bracketed by the two models, although the Nb rates approach more closely to the ZRP limit.

As a single parameter measure of the multielectron contribution to the suppression of ionization via the dynamic polarizability, we propose the following:

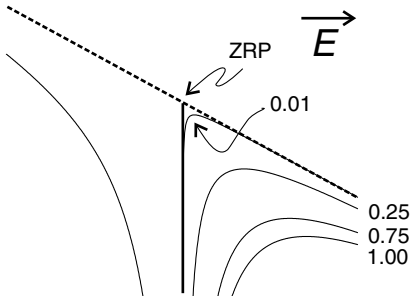

FIG. 3. Adiabatic multielectron polarization in a strong laser field leads to displacement of electron density towards the barrier. This leads to enhanced screening of the core as viewed from the downfield region. We mimic the enhanced downfield screening through the use of an effective Coulomb charge z. For an unscreened core of unit charge $z = 1$, reduction in z (i.e., more core screening) mimics the field-induced modification of the tunneling barrier, as can be seen for $z = 0.75$, 0.25, and 0.01. In the limit $z \to 0$, the potential tends towards a delta or ZRP.

$$\eta = \frac{I_{\mathrm{sat}}(\mathrm{Exp}) - I_{\mathrm{sat}}(\mathrm{ADK})}{I_{\mathrm{sat}}(\mathrm{ZRP}) - I_{\mathrm{sat}}(\mathrm{ADK})}.$$

The value η is a number between zero and one. A number close to 0 denotes good agreement with ADK theory and a single active electron picture of the ionization dynamics (hence, $\eta = 0$ for Xe). A value close to 1 denotes good agreement with the ZRP model which we suggest is indicative of strong multielectron contributions to the dynamic polarization, leading to dramatic suppression of ionization rates. It is important to note that η is defined in terms of the saturation intensities (as in Fig. 1) and not from the absolute ionization rates (as in Fig. 2). As can be seen from Table I, except for Nb, all these atoms show a value of η around 0.2, indicating some multielectron contributions to the dynamic screening. Interestingly, these appear to be invariant with respect to the total number of valence electrons or the static polarizability. For Nb, by contrast, $\eta = 0.5$ represents a very strong dynamic screening effect. This anomalous behavior is currently under further investigation in our laboratory, but several indications of the unusual polarizability of Nb and its clusters have been documented in the literature [21,22].

In conclusion, the strong field ionization dynamics of the multielectron atoms V, Nb, Ta, Ni, and Pd have been investigated in the adiabatic (infrared) limit. We reported absolute ionization rates and saturation intensities that are independent of experimental parameters and, hence, are directly comparable with theory. We observed a strong suppression of ionization, as compared with single active electron theory expectations. We ascribed this effect to multielectron dynamic screening, related to the multielectron contribution to the polarizability of the system, analogous to what was discussed in the strong field ionization of C_{60} [23] and metal clusters [24]. The latter systems were described in terms of a classical conducting sphere model, successful in treating larger systems such as clusters of ten or more metal atoms, but which does not apply to small quantum systems: classical models fail to describe the polarizability of single atoms. We have bracketed the absolute ionization rates of the atoms investigated here between, on the one hand, a SAE model (ADK) and, on the other hand, a simple model which we propose behaves as the high dynamic screening limit—the ZRP. In strong fields, even material systems as simple as isolated atoms can exhibit a richness that transcends the simple physics of one electron systems. We hope that these results will encourage the further development of full many-body quantum mechanical theories of strong field ionization.

The authors thank T. Brabec (University of Ottawa) and E. Zaremba (Queen's University) and especially M.-Yu. Ivanov (NRC) for valuable discussions.

*Electronic address: albert.stolow@nrc-cnrc.gc.ca
†Electronic address: david.rayner@nrc-cnrc.gc.ca

[1] M. V. Ammosov *et al.*, Sov. Phys. JETP **64**, 1191 (1986).
[2] B. Walker *et al.*, Phys. Rev. Lett. **73**, 1227 (1994).
[3] P. B. Corkum, Phys. Rev. Lett. **71**, 1994 (1993).
[4] G. D. Gillen and L. D. Van Woerkom, Phys. Rev. A **68**, 33 401 (2003).
[5] M. Sukharev *et al.*, Phys. Rev. A **66**, 53 407 (2002).
[6] S. M. Hankin *et al.*, Phys. Rev. Lett. **84**, 5082 (2000).
[7] S. M. Hankin *et al.*, Phys. Rev. A **64**, 013405 (2001).
[8] M. Lezius *et al.*, Phys. Rev. Lett. **86**, 51 (2001).
[9] M. Lezius *et al.*, J. Chem. Phys. **117**, 1575 (2002).
[10] M. J. DeWitt *et al.*, Phys. Rev. Lett. **87**, 153001 (2001).
[11] X. M. Tong *et al.*, Phys. Rev. A **66**, 033402 (2002).
[12] J. Muth-Bohm *et al.*, Phys. Rev. Lett. **85**, 2280 (2000).
[13] J. Zanghellini *et al.*, J. Phys. B **37**, 763 (2004).
[14] Ch. Fabian *et al.*, J. Mod. Opt. **50(3-4)**, 589 (2003).
[15] M. Smits *et al.*, Rev. Sci. Instrum. **74**, 4812 (2003).
[16] S. Lochbrunner *et al.*, J. Electron Spectrosc. Relat. Phenom. **112**, 183 (2000).
[17] S. G. Lias and J. F. Liebman, in *NIST Chemistry WebBook, NIST Standard Reference Database Number 69*, edited by P. J. Linstrom and W. G. Mallard (NIST, Gaithersburg, Maryland, 2003); also available at http://webbook.nist.gov.
[18] T. M. Miller, in *Handbook of Chemistry and Physics*, edited by D. Lide (CRC Press, Boca Raton, 2003), 84th ed.
[19] G. Yudin and M. Ivanov, Phys. Rev. A 64 **64**, 013409 (2001).
[20] A. M. Perelomov *et al.*, Sov. Phys. JETP **23**, 924 (1965).
[21] R. Moro *et al.*, Science **300**, 1265 (2003).
[22] M. B. Knickelbein, J. Chem. Phys. **118**, 6230 (2003).
[23] V. R. Bhardwaj *et al.*, Phys. Rev. Lett. **91**, 203004 (2003).
[24] M. Smits *et al.*, Phys. Rev. Lett. **93**, 203402 (2004).